Vacuum-enhanced nickel-induced crystallization of hydrogenated amorphous silicon

N. Budini,[1,a)] P. A. Rinaldi,[1] R. D. Arce,[1,2] J. A. Schmidt,[1,2] R. R. Koropecki,[1,2] and R. H. Buitrago[1,2]

[1]*Instituto de Desarrollo Tecnológico para la Industria Química, UNL-CONICET, Güemes 3450, S3000GLN Santa Fe, Argentina*

[2]*Facultad de Ingeniería Química, UNL, Santiago del Estero 2829, S3000AOM Santa Fe, Argentina*

(Received 30 June 2012; accepted 5 September 2012; published online 4 October 2012)

We report the results of enhanced nickel induced crystallization of intrinsic hydrogenated amorphous silicon thin films under vacuum conditions. Crystallization was performed by conventional furnace annealing at both atmospheric pressure and vacuum or low pressure conditions ($\approx 10^{-6}$ Torr) for comparison. We have investigated the influence of low pressure during annealing on the resulting polycrystalline films by means of optical microscopy, ultraviolet reflectance, and photoacoustic spectrometry measurements. A faster crystallization and a smaller grain size were observed when the process is carried out under vacuum, with an annealing time reduction of more than 50%. We discuss, from a thermodynamical viewpoint, some possible causes by which vacuum annealing influences incubation and nucleation stages due to the presence of mobile hydrogen atoms inside the amorphous silicon matrix. Large grains with diameters of 30 and 100 μm were obtained at vacuum and atmospheric pressure, respectively. © *2012 American Institute of Physics*. [http://dx.doi.org/10.1063/1.4757574]

I. INTRODUCTION

Polycrystalline silicon (pc-Si) thin films have been intensively studied along the last two decades. Their applications in micro- and large-area-electronic devices, such as thin film transistors (TFT) and solar cells, have grown considerably.[1,2] The pc-Si films can be obtained from a relatively inexpensive hydrogenated amorphous silicon (a-Si:H) film, deposited by plasma-enhanced chemical vapor deposition (PECVD), after a suitable thermal annealing process.[3] Several processes have been proposed and thoroughly investigated in order to crystallize a-Si:H in the most efficient way.[2] Among them, the most simple and common is solid phase crystallization (SPC), which can be accomplished by conventional furnace annealing (CFA).[2–4] To avoid contamination of the sample with reactive impurities, mainly oxygen, the annealing is generally carried out under a constant flux of an inert gas such as nitrogen or argon. This provides a clean ambient while keeping the furnace at atmospheric pressure (AP) during SPC (AP-SPC from now on). The main drawbacks of AP-SPC are the requirement of long annealing periods and the relatively small grain size achieved, yielding nano- or micro-crystalline silicon thin films.[4,5] Metal induced crystallization (MIC)[6] appeared as a convenient technique to increase the final grain size while reducing the AP-SPC annealing temperature. Although MIC methods provide pc-Si thin films with grain sizes above 10 μm, if Ni is used as the metallic catalyst the annealing periods of AP-SPC by CFA are not appreciably shortened.[7] Some authors have used rapid thermal annealing (RTA) instead of CFA to accomplish AP-SPC of a-Si:H, in order to obtain ultra-thin (<100 nm) pc-Si films after shorter annealing periods of several minutes.[6,8]

In previous works we have studied MIC induced by Ni (or NIC, from nickel induced crystallization).[7,9,10] It is known that the addition of very small amounts of Ni ($\sim 10^{14}$–10^{15} at./cm^2) to the a-Si:H film surface induces the growth of large grains after AP-SPC at temperatures below 600 °C. NIC proceeds by the formation of Ni-disilicide ($NiSi_2$) nuclei after thermally activated diffusion of Ni atoms, previously deposited on top of the a-Si film.[8–11] The formation of $NiSi_2$ nuclei creates a Ni-depleted zone around them and a crystallization front starts to advance in the surrounding amorphous material.[12] This is possible because Ni atoms in the $NiSi_2$/a-Si interface lower their energy by diffusing to the a-Si network and reacting to form a new $NiSi_2$/a-Si crystallization front.[13] Since the lattice parameter of $NiSi_2$ differs by only 0.4% to that of single-crystalline silicon (c-Si), Si atoms that are left behind after Ni diffusion can rearrange themselves to form a c-Si network.[11] This process is not endless and is limited by the fact that the amount of Ni atoms decreases as long as the crystallization front advances. It is also known that certain density of Ni atoms remains trapped at the c-Si network although a higher density is always present at the advancing front.[14] Therefore, crystallization continues until Ni concentration in the crystallization front is sufficiently reduced or until neighbouring grains collide. This procedure allows achieving pc-Si films with grain sizes above 100 μm after annealing for periods longer than 24 h. However, the effect of vacuum or low pressure (indistinctly vacuum or LP from now on) annealing on NIC of a-Si:H has not been systematically investigated to date nor compared to AP-SPC. Recently, Shanavas *et al.*[15] have studied the crystallization of non-hydrogenated a-Si at high pressures by means of classical molecular dynamics

a)Author to whom correspondence should be addressed. Electronic mail: nbudini@intec.unl.edu.ar.

simulations, being one of scarce works we could find concerning the influence of pressure on crystallization of a-Si (or its alloys). They have found that high pressure regimes have a direct impact on crystallization temperature.

In this work we report experimental results concerning NIC of a-Si:H by means of SPC at LP as compared to AP-SPC, featuring drastically reduced annealing periods for obtaining pc-Si thin films with considerably large grain sizes. Also, we discuss a possible cause of vacuum-enhanced NIC of a-Si:H in relation with evidence gathered from optical microscopy (OM), ultraviolet (UV) reflectance, infrared (IR) transmittance, and photoacoustic spectrometry (PAS) measurements.

II. EXPERIMENTAL DETAILS

We deposited 350 nm-thick intrinsic a-Si:H samples on Schott AF-37 glass in a capacitively coupled PECVD reactor operating at a frequency of 50 MHz and a power density of 120 mW/cm^2. The reactive gas was pure silane (SiH_4). The substrate temperature during deposition was set at 200 °C and the gas pressure was 0.45 Torr, leading to a deposition rate of 15–20 Å/s. Ni was subsequently deposited on top of the films by dc-sputtering, leading to surface atomic densities of $\sim 10^{14}$ at./cm^2. A conventional tubular furnace was conditioned in order to allow the simultaneous SPC of the samples at AP and LP regimes. A turbomolecular pump was connected to the vacuum branch of the setup, allowing a final pressure of about 10^{-6} Torr. The AP branch was maintained under a N_2 flow of 20 sccm to provide an inert atmosphere. The samples were kept at the same transversal position of the furnace to ensure the same temperature during annealing. This was checked by two thermocouples, one at each branch, differing by less than 3 °C which can be practically neglected. After a dehydrogenation step at 420 °C, samples were annealed for 24 h at 580 °C.

In order to get insights on the mechanisms favoring crystallization during SPC under vacuum we have carried out OM, UV reflectance, IR transmittance, and PAS measurements. OM images, obtained with a digital camera attached to an Olympus DX-50 microscope, were used to calculate the crystalline fraction (X_c) and the average grain size (D). From UV reflectance spectra, obtained in a Shimadzu UV-3600 spectrometer, we have confirmed the crystallization of the films and obtained the crystallinity (ΔR) and crystalline quality (Q) parameters, which quantify the similarity of the sample spectrum to that of c-Si.

IR transmittance measurements were carried out in a Nicolet 8700 FTIR spectrometer to follow the evolution of the hydrogen content inside the films with thermal annealing. This allows inspecting for differences in the effusion rate of hydrogen from the samples under different pressure conditions, which may act as a nucleation inductor. Measurements were performed on equivalent a-Si:H samples deposited onto c-Si in order to have a suitable background for the spectra, after annealing at 400 and 500 °C stages.

On the other hand, we have studied the variations of the PAS signal of the films, induced by thermal annealing at AP and LP regimes. The PAS technique allows determining some important parameters such as the heat capacity (C_p), which is useful for a thermodynamical analysis of crystallization. To carry out PAS measurements we deposited 500 nm-thick a-Si:H samples under the same conditions as before. The annealing process was performed at AP and LP and consisted in isochronic stages of 6 h at the following temperatures: 400, 415, 430, 445, 460, 475, and 500 °C. Measurements were performed after each stage in order to inspect the evolution of C_p, allowing us to calculate the excess entropy (ΔS), the enthalpy (ΔH), and the free energy (ΔG) at the beginnings of the crystallization process (i.e., at the incubation stage, prior to nucleation). We have evaluated and compared the results obtained in both regimes (AP and LP) in order to have a clue about the way in which vacuum conditions favors NIC process on a-Si:H.

III. RESULTS AND DISCUSSION

A. UV reflectance and OM results

As a first result of our work, the annealing process at 580 °C during 24 h resulted in a fully crystallized sample at LP and a partially crystallized sample at AP. The crystalline fraction, X_c, of the AP sample was estimated to be of 71% by OM measurements. Fig. 1 shows an OM transmission image of this sample. The transitory mean grain size or diameter, D, was calculated from Fig. 1 (left-side inset) and resulted in $D = (99.1 \pm 8.7)$ μm at this intermediate state of crystallization. Hence, it is expected that the final grain size will be around 100 μm. The right-side inset of Fig. 1 shows an amplified image of colliding grains, which give rise to well-defined grain boundaries. In contrary to AP, the crystallization under vacuum was completed but the final grain size was quite lower. A mean final grain size of $D = (26.7 \pm 3.0)$ μm was obtained from OM measurements.

Fig. 2 presents the UV reflectance spectra of samples annealed at LP and AP during 24 h. This figure also presents the spectra corresponding to c-Si and a-Si:H, for comparison. The usefulness of UV reflectance comes from the fact that c-Si shows two characteristic peaks at $\lambda = 274$ and 365 nm,

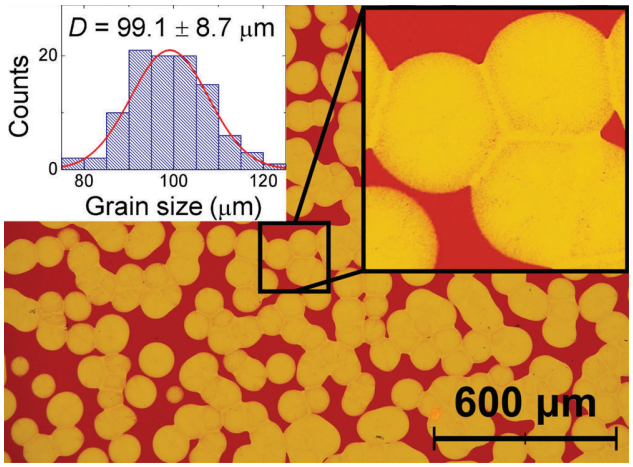

FIG. 1. OM transmission image of the sample crystallized at the AP regime after 24 h. The calculated crystallized fraction is $X_c = 71\%$. The insets show (left-side) the grain size histogram, with a transitory mean diameter of 99.1 μm, and (right-side) a grain boundary in higher detail.

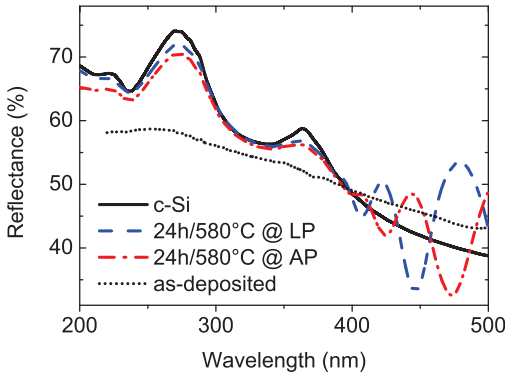

FIG. 2. UV reflectance spectra of samples annealed at LP (dashed curve) and at AP (dash-dotted). Both spectra show crystallization signs and are compared to c-Si spectrum (solid curve) and as-deposited (dotted curve) spectrum.

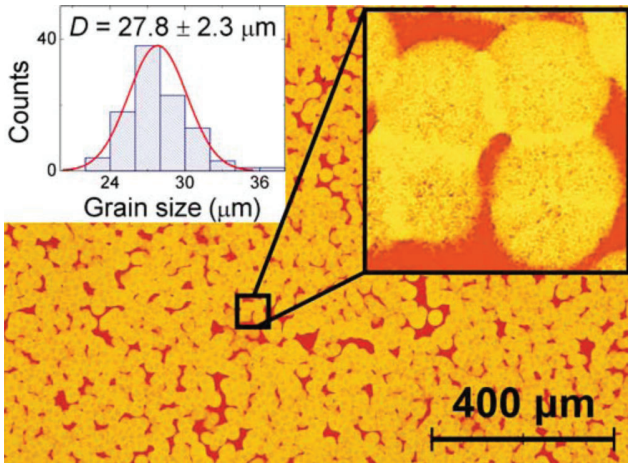

FIG. 3. OM transmission image of the sample crystallized at the LP regime after 6 h. The calculated crystallized fraction is $X_c = 87.7\%$. The insets show (left-side) the grain size histogram, with a transitory mean diameter of 27.8 μm, and (right-side) a grain boundary in higher detail.

approximately, which correspond to optical interband transitions at the X point (band E_2) and along the Γ–L axis (band E_1) of the Brillouin zone, respectively.[16] Thus, the presence of these transitions in the samples ensures the existence of crystallized material. By comparing the measured spectra to that of c-Si it is possible to roughly estimate the "crystalline quality", Q, and the "crystallinity", ΔR, of the film by means of the following expressions[17]

$$Q = \frac{1}{2}\left[\frac{R_1}{R_1^{\text{c-Si}}} + \frac{R_2}{R_2^{\text{c-Si}}}\right], \tag{1}$$

$$\Delta R = \frac{R_1 - R_2}{R_1^{\text{c-Si}} - R_2^{\text{c-Si}}}, \tag{2}$$

where R_1 and R_2 are the heights of the peaks at $\lambda = 274$ and 365 nm, respectively, and the "c-Si" superscript refers to the analogous values of the c-Si reference spectrum. The quantity Q is a figure of merit which quantifies how similar is the sample spectrum to that of c-Si, being them identical for $Q = 1$. The definition of ΔR is based on the fact that the peak centered at 274 nm is influenced by roughness and crystallinity, while the lower energy peak centered at 365 nm accounts mainly for roughness. These parameters are generally used to determine the surface quality of pc-Si films, where a deviation from the c-Si spectrum is associated to the lack of long-range order in the material.[18]

From UV reflectance results we obtained values above $Q = 0.95$ and $\Delta R = 0.93$, for both samples, regardless of the pressure during annealing. However, the spectra corresponding to the samples annealed under vacuum result systematically more likely to that of c-Si, as is shown in the particular case of Fig. 2. The high Q and ΔR values obtained reveal a high crystallinity and crystalline quality of the films.

To investigate the evolution of crystallization under vacuum and to estimate the annealing time required for full crystallization we experimented with shorter annealing periods. As a result, after a 6 h annealing at 580 °C under vacuum the crystallized fraction of the sample was $X_c = 88\%$ and the transitory mean grain size was $D = (27.8 \pm 2.3)$ μm, as can be seen in Fig. 3, which indicates that the final grain size will not be too different. The insets show, as before, the grain size histogram (left-side) and a zoomed image presenting the grain boundary formation (right-side). This result is in clear agreement with that obtained for the sample annealed under vacuum during 24 h, since the final grain sizes are comparable inside the experimental error in both cases. As can be seen from Figs. 1 and 3, the grains obtained at AP look more compact and with better defined boundaries whereas at LP the boundaries present some dendritic branches although the disk shape is conserved. From the above results we conclude that full crystallization was achieved soon after a 6 h annealing period under vacuum conditions.

In order to ensure this conclusion, the vacuum annealing was extended for a 6 h period, resulting in a 12 h total annealing time at 580 °C. After this, the crystallization was completed ($X_c \approx 100\%$) and the final grain size was $D = (25.3 \pm 2.6)$ μm. The final grain size after 24 and 12 h remains almost the same than the transitory grain size after 6 h, calculated from Fig. 3, indicating that full crystallization was effectively achieved between 6 and 12 h of vacuum annealing at 580 °C, as previously hypothesized.

Fig. 4 presents the evolution of the UV reflectance spectrum from the as-deposited (amorphous) state to the crystallized state after a 12 h annealing under vacuum. The 6 h curve reveals crystalline peaks with $Q = 0.94$ and $\Delta R = 0.77$. After 12 h, the measured spectrum was enhanced, having $Q = 0.98$ and $\Delta R = 0.91$, and mimicked better the c-Si curve revealing that crystallization has effectively continued. Hence, full crystallization of the sample was achieved after an annealing period ranging from 6 to 12 h (i.e., less than 12 h), at 580 °C and at a pressure of 10^{-6} Torr.

Neglecting the incubation period and supposing that grains nucleate altogether, one can estimate roughly the average grain growth velocity, v_g, by means of the quotient between the transitory mean grain size, D, and the elapsed annealing time, t_{ann}, i.e.,

$$v_g = \frac{D}{t_{ann}}. \tag{3}$$

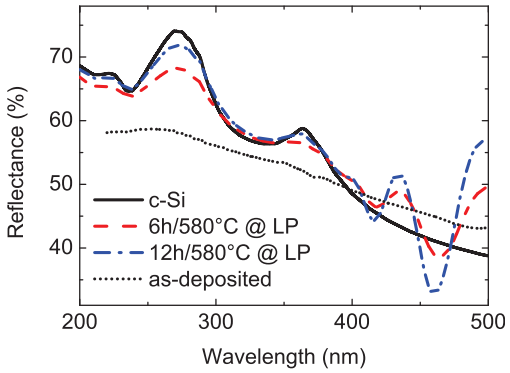

FIG. 4. UV reflectance spectra of a sample annealed at LP at three different stages of crystallization: (dotted curve) amorphous, (dashed curve) partially crystallized after 6 h at 580 °C and (dash-dotted) fully crystallized after 12 h at 580 °C. The c-Si spectrum (solid curve) is also presented as reference.

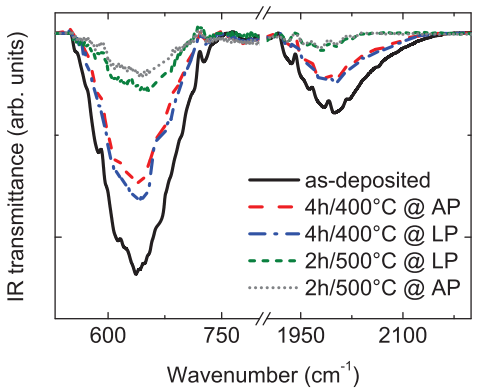

FIG. 5. IR transmittance spectra of samples annealed simultaneously at AP and LP. The hydrogen content in the samples evolves almost at the same rate in both regimes, and the effect of pressure on hydrogen effusion appears to be negligible.

In this way, for AP annealing after 24 h the mean grain size was 99.1 μm and thus $v_g = 4.1$ μm/h, while for LP annealing after 6 h, with $D = 27.8$ μm, one obtains $v_g = 4.6$ μm/h. Therefore, besides the fact that full crystallization was achieved faster under vacuum, it is well worth to remark that the average grain growth velocity was roughly the same in both cases. This similarity allows discerning that the difference between LP and AP crystallization may come from the incubation/nucleation stage and not from the growth stage. Another clear evidence of this is the higher nuclei density observed at vacuum, which finally led to a smaller grain size, indicating a different behavior at the initial stages of crystallization. In order to discard any oxygen induced effect due to unwanted impurities, we have based on the results obtained by Lin *et al.*[19] They have found that the annealing atmosphere (oxygen or nitrogen in their study) does not influence the lateral growth rate in NIC at AP. Also, they have observed that oxygen incorporated into the films previously to annealing (in the form of NiO) affects the incubation/nucleation process in the same way regardless of the atoms present in the annealing ambient.

B. FTIR results

Due to the relatively high initial hydrogen concentration of the films, which is in the range of 10–15 at. %,[4] and being based on the fact that hydrogen induces nucleation,[4,20] we tried to look for any differences in the hydrogen effusion rates from the samples due to the pressure difference during annealing, which may be responsible of favoring the incubation/nucleation of $NiSi_2$ precipitates under vacuum. The evolution of the IR transmittance spectra of equivalent samples annealed at AP and LP, at 400 °C for 4 h and after at 500 °C for 2 h, is presented in Fig. 5. In their initial as-deposited state both spectra are identical and only one of them is presented for clearness. Moreover, after each stage of annealing there were no significant differences between both regimes, despite one was tempted to expect a higher effusion under vacuum. This result is in agreement with that of Beyer *et al.*[21,22] who have intensively studied the hydrogen effusion in a-Si:H and other materials, concluding that it is a diffusion limited process which should not be influenced by an external pressure drop.

We have presented enough evidence indicating that the incubation/nucleation stages of the NIC process are enhanced at vacuum. These evidences are lower annealing times to achieve full crystallization, a higher amount of grains per unit area and, consequently, a diminished grain size. Also, the similarity of the average grain growth velocity between AP and LP regimes constitutes evidence supporting the influence of vacuum on the initial stages of crystallization. However, hydrogen effusion does not seem to be the responsible of influencing nucleation. In the following section we present results obtained from PAS measurements, which may put some light into the problem.

C. PAS results

From a thermodynamic viewpoint, the heat capacity at constant pressure is related to thermal diffusivity simply as[23]

$$C_p = \frac{k}{\alpha}, \tag{4}$$

where k is the thermal conductivity and α the thermal diffusivity of the material. In the case of a-Si:H, k can be considered constant and equal to 1.7 W m^{-1} °C^{-1} in the range between room temperature and 500 °C, which is the range we have used to study the incubation/nucleation stage. Thus, C_p can be determined from PAS measurements since α is a fitting parameter in the classical approach to PAS theory developed by Hu *et al.*[24] The relevance of knowing C_p resides in the fact that phase transitions are generally characterized by an abrupt change in C_p.

We performed at first a thermodynamic interpretation of the thermal process through an analysis of the enthalpy change $dH = d(U + PV) = dQ + VdP$, where U is the internal energy of the system, P and V are the pressure and volume, respectively, and dQ is the amount of heat absorbed ($=TdS$). The heat capacity, C_p, in accordance with previous formulation can be also expressed as[25]

$$C_p = \left(\frac{dQ}{dT}\right)_p = \left(\frac{dH}{dT}\right)_p, \tag{5}$$

since $VdP = 0$ at constant pressure. In this way, the combination of Eqs. (4) and (5) allows to calculate the enthalpy change during annealing at constant pressure.

Despite the fact that this is an irreversible process in which the PV work is negligible ($dV/dT \approx 0$) or $\Delta H \approx \delta Q_{irr}$ (where δQ_{irr} stands for irreversibly absorbed heat), the a-Si:H film increases its enthalpy because the incubation is not a spontaneous reaction and, therefore, ΔH should be positive. For simplicity, we take $H_0(P_0, T_0) = 0$. Thus, ΔH corresponds to an activation energy, which is needed to reach the incubation and nucleation of crystalline nuclei. This produces a change in C_p during annealing and gives place to a *glass transition*, at temperatures near 420 °C. The variation of C_p with annealing at AP and LP is presented in Fig. 6, together with the enthalpy changes at both regimes. It is known that in this kind of transition there is neither volume change nor latent heat.[26] This implies that the entropy is a continuous function around the transition point.

According to Remes *et al.*,[27] the mass density of a-Si:H obtained by different deposition methods decreases for higher hydrogen concentrations. It has been shown that a reconstruction of the Si–Si bonds at about 430 °C leads to a slight thickness diminution and a density increment of about 3% for hydrogen concentrations around 9 at. %. However, this change in density does not explain the observed variation of C_p. The metastability in a-Si:H favors a rearrangement of Si–Si bonds and principally of Si–H bonds at a widespread level.

By placing the samples under vacuum, a negative PV work is done. Hence, in this case the initial enthalpy is lower than at AP (i.e., $H^0_{LP} < H^0_{AP}$) and, therefore, the relation $\Delta H_{LP} > \Delta H_{AP}$ holds. In both cases, the values of the slope dH/dT give as a result a rapid change in C_p as shown in Fig. 6.

The excess entropy is one of the most important thermodynamic extensive parameters, being useful to inspect and quantify processes taking place far from equilibrium conditions, as would be the case of the transformation of a material from its amorphous state to a crystallized one. In particular, the relation between entropy and the change of C_p due to a thermal induced microstructural evolution is

$$\Delta S = S_{\text{a-Si:H}} - S_{\text{c-Si}} = \int (C_p^{\text{a-Si:H}} - C_p^{\text{c-Si}}) \frac{dT}{T}, \tag{6}$$

where emphasis is done in the fact that for the calculations we have taken as a reference the known values for c-Si, as denoted by the "c-Si" and "a-Si:H" superscripts.

Vacuum annealing results in a less abrupt change of C_p, yielding $\Delta S_{LP} > \Delta S_{AP}$, as can be seen in Fig. 7. Thus, the entropy during dehydrogenation at LP results to be higher than at AP, increasing the structural disorder by means of the formation and redistribution of Si–H bonds. This may favor the formation of $NiSi_2$ nuclei under vacuum, since it is well known that disorder and H mobility induce nucleation and, consequently, crystallization.[4,28] It is worth noting here that this does not imply a faster H effusion at vacuum, which is mediated by surface desorption, but only a higher H mobility or diffusion inside the amorphous matrix induced by vacuum. In this way, Si–H bonds can be thought as "solidifying" to a glassy phase, which upon reaching a new equilibrium state causes an entropy drop. Also, the maxima of the curves are located near 420 °C, which is thought to be the glass transition temperature. One point should be made clear here, which is that although the second law of thermodynamics says that $T\Delta S > \delta Q_{irr}$, we got $T\Delta S < \Delta H$. However, this is not a contradiction since we have used the c-Si (i.e., the more ordered, or lower entropy, state) as a reference for the calculations. Another implication of the second law is that the entropy of an isolated system tends to increase with time and, in this sense, higher entropy values under vacuum (as seen in Fig. 7) would indicate a time gain for crystallization at the expense of heating and reducing the pressure of the system.

With the previous gathered information, we can estimate the Gibbs free energy which is defined as $\Delta G = \Delta H - T\Delta S$. This is a quantity of great importance in chemical processes at constant pressure. As said before, it is possible to distinguish two different processes concerning hydrogen mobility: (i) H rearrangement by internal diffusion (ii) H effusion by surface desorption. The results obtained for the free energy

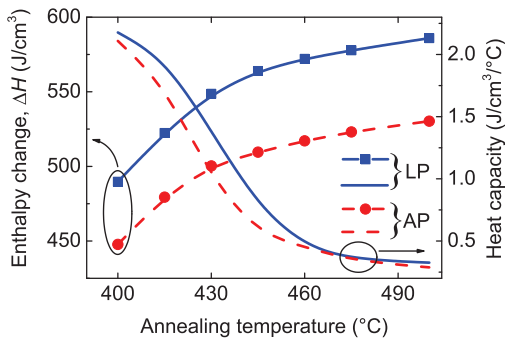

FIG. 6. Enthalpy change calculated from PAS measurements after annealing stages of 6 h at temperatures in the 400–500 °C range, at (dashed curve) AP and (solid curve) LP. The $C_p = (dH/dT)_p$ curves are also presented. Systematically higher values are obtained for ΔH at the LP regime.

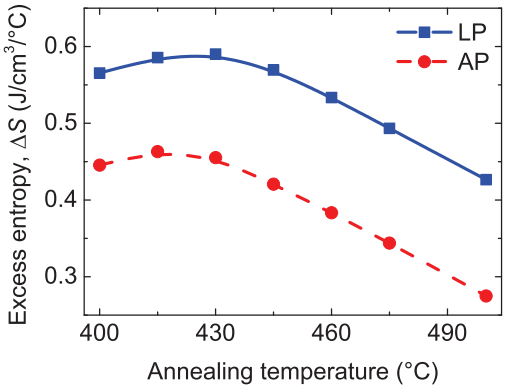

FIG. 7. Evolution with annealing of the excess entropy curves obtained from PAS measurements. The higher values observed under vacuum are responsible of increasing the structural disorder through Si–H bonds redistribution, inducing nucleation by H mobility.

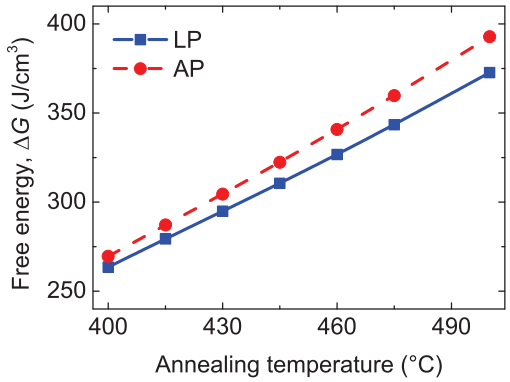

FIG. 8. Change in free energy after the 6 h annealing stages at temperatures in the 400–500 °C range, at AP and LP. The slight difference between both regimes may be due to a change in the diffusion coefficient of hydrogen inside the a-Si:H matrix at lower pressures.

calculations are shown in Fig. 8. We consider that the increment of ΔG with the annealing sequence is mainly due to H effusion, which is observed both at AP and LP.

From this analysis, and taking into account our previous conclusion of an equal effusion rate at both regimes, we can infer that the H mobility within the sample is rather different (higher) at LP than at AP. This may be due to a variation (increment) of the H diffusion coefficient, induced by the pressure difference of about six orders of magnitude. According to the general Arrhenius model for diffusion coefficient, i.e., $D_H = D_0 \exp(-E_a/kT)$ in the present case, we may assert from our experiments that E_a is pressure dependent and decreases as pressure diminishes. However, according to the Meyer-Neldel rule,[29] D_H could also depend on pressure. This analysis exceeds the scope of the present work and would need further study but, in any case, D_H seems to vary with pressure during annealing as ΔG does. The *extended hydrogen glass* model[30] assumes that weak Si–Si bonds are reconfigured on a local scale due to H diffusion inside the a-Si:H matrix, which may be the reason of the slight difference between ΔG at LP and at AP as seen in Fig. 8.

In our previous works concerning NIC of a-Si:H[7,9,10] we have obtained fully crystallized films only after 24 h, and generally near 48 h, of AP-SPC at 580 °C. Thus, the results obtained in this investigation represent an advance in the direction of crystallization time reduction by means of vacuum annealing. We state that despite the final grain size reduction of about 60%, a considerable annealing time reduction greater than 50% is advantageous for practical purposes. A lower grain size is generally related to a greater defect density at grain boundaries which are detrimental for the electrical performance of the material. However, considering the application of these pc-Si thin films for TFT or solar cell devices, the final grain size is still adequately large if compared to other works in this field.[7,31,32] Also, proper passivation of grain boundaries can greatly avoid the prejudicial effect of this defective zone on the electric transport.[33]

IV. CONCLUSION

In summary, NIC of a-Si:H thin films is enhanced by CFA at pressures of about 10^{-6} Torr. In comparison to crystallization at AP in an inert ambient, the final grain size is lower but still relatively large, of about 30 μm. Since the average grain growth rate was found to be nearly the same at both regimes, we conclude that the pressure settled during annealing influences the incubation/nucleation stages and not the growth stage. From the analysis of hydrogen effusion rate by means of infrared transmittance, no important differences were found between LP and AP which is in accordance with previous results from other authors. In this way, the mechanism by which the formation of $NiSi_2$ nuclei—and therefore crystallization—is enhanced under vacuum is attributed to a faster hydrogen inner diffusion and redistribution of Si–H bonds at lower pressures. This is consistent with the well-known nucleation induction caused by mobility of hydrogen atoms and was evidenced by PAS measurements and/or calculation of thermodynamical parameters, which showed a systematic difference between annealing at LP and at AP. Reduction of grain size and crystallization time support the conclusions attained so far. Further research is being done in order to get a better understanding of this phenomenon.

ACKNOWLEDGMENTS

This work was funded by CONICET projects PIP-1464 and CAI + D-68-349.

[1]R. B. Iverson and R. Reif, J. Appl. Phys. **62**, 1675 (1987).
[2]A. G. Aberle, Thin Solid Films **511/512**, 26 (2006).
[3]J. K. Rath, Sol. Energy Mater. Sol. Cells **76**, 431 (2003).
[4]N. Budini, P. A. Rinaldi, J. A. Schmidt, R. D. Arce, and R. H. Buitrago, Thin Solid Films **518**, 5349 (2010).
[5]D. Song, D. Inns, A. Straub, M. L. Terry, P. Campbell, and A. G. Aberle, Thin Solid Films **513**, 356 (2006).
[6]S. Y. Yoon, S. J. Park, K. H. Kim, and J. Jang, Thin Solid Films **383**, 34 (2001).
[7]J. A. Schmidt, N. Budini, P. A. Rinaldi, R. D. Arce, and R. H. Buitrago, J. Cryst. Growth **311**, 54 (2008).
[8]C. F. Cheng, T. C. Leung, M. C. Poon, C. W. Kok, and M. Chan, IEEE Trans. Electron Devices **51**, 2205 (2004).
[9]J. A. Schmidt, N. Budini, P. A. Rinaldi, R. D. Arce, and R. H. Buitrago, J. Phys.: Conf. Ser. **167**, 012046 (2009).
[10]J. A. Schmidt, N. Budini, R. D. Arce, and R. H. Buitrago, Phys. Status Solidi C **7**, 600 (2010).
[11]F. A. Ferri, A. R. Zanatta, and I. Chambouleyron, J. Appl. Phys. **100**, 094311 (2006).
[12]C. Hayzelden and J. L. Batstone, J. Appl. Phys. **73**, 8279 (1993).
[13]A. R. Joshi, T. Krishnamohan, and K. C. Saraswat, J. Appl. Phys. **93**, 175 (2003).
[14]M. Wong, Z. Jin, G. A. Bhat, P. Wong, and H. S. Kwok, IEEE Trans. Electron Devices **47**, 1061 (2000).
[15]K. V. Shanavas, K. K. Pandey, N. Garg, and S. M. Sharma, J. Appl. Phys. **111**, 063509 (2012).
[16]G. Harbeke and L. Jastrzebski, J. Electrochem. Soc. **137**, 696 (1990).
[17]A. Straub, P. I. Widenborg, A. Sproul, Y. Huang, N. Harder, and A. G. Aberle, J. Cryst. Growth **265**, 168 (2004).
[18]D. Dimova-Malinovska, O. Angelov, M. Sendova-Vassileva, and V. Mikli, J. Optoelectron. Adv. Mater. **11**, 1079 (2009), available at http://joam.inoe.ro/index.php?option=magazine&op=view&idu=2030&catid=42.
[19]Y.-D. Lin, Y.-C. S. Wu, C.-W. Chao, and G.-R. Hu, Mater. Chem. Phys. **80**, 577 (2003).
[20]C. Godet, N. Layadi, and P. R. i Cabarrocas, Appl. Phys. Lett. **66**, 3146 (1995).
[21]W. Beyer, Physica B **170**, 105 (1991).
[22]W. Beyer and F. Einsele, "Hydrogen effusion experiments," in *Advanced Characterization Techniques for Thin Film Solar Cells*, edited by D. Abou-Ras, T. Kirchartz, and U. Rau (Wiley-VCH Verlag GmbH & Co., 2011).

[23]C. Kittel, *Introduction to Solid State Physics*, 7th ed. (Wiley & Sons, 1996).
[24]H. Hu, X. Wang, and X. Xu, J. Appl. Phys. **86**, 3953 (1999).
[25]M. Zemansky, *Heat and Thermodynamics* (Aguilar, 1990).
[26]C. A. Angell, K. L. Ngai, G. B. McKenna, P. F. McMillan, and S. W. Martin, J. Appl. Phys. **88**, 3113 (2000).
[27]Z. Remeš, M. Vaněček, A. H. Mahan, and R. S. Crandall, Phys. Rev. B **56**, R12710 (1997).
[28]A. Hadjadj, N. Pham, P. R. i Cabarrocas, O. Jbara, and G. Djellouli, J. Appl. Phys. **107**, 083509 (2010).
[29]W. Meyer and H. Neldel, Z. Tech. **18**, 588 (1937).
[30]D. P. Masson, A. Ouhlal, and A. Yelon, J. Non-Cryst. Solids **190**, 151 (1995).
[31]H.-Y. Chu, M.-Y. Chiang, L. Yiz, and S.-H. Zhou, in Proceedings of 6th IEEE International Conference on Nano/Micro Engineered and Molecular Systems, Taiwan, 20-23 February 2011, p. 1040.
[32]D. Van Gestel, I. Gordon, and J. Poortmans, Phys. Proc. **11**, 196 (2011).
[33]Y. Tao, S. Varlamov, G. Jin, M. Wolf, and R. Egan, Thin Solid Films **520**, 543 (2011).